ELSEVIER

Sensors and Actuators A 103 (2003) 231–236

SENSORS AND ACTUATORS A PHYSICAL

www.elsevier.com/locate/sna

A micromachined RF microrelay with electrothermal actuation☆

Ye Wang[a,b,*], Zhihong Li[a,c], Daniel T. McCormick[a,b], Norman C. Tien[a]

[a]*Department of Electrical and Computer Engineering, Berkeley Sensor and Actuator Center, University of California at Davis, Davis, CA 95616, USA*

[b]*Department of Electrical and Computer Engineering, Cornell University, Ithaca, NY 14853, USA*

[c]*Institute of Microelectronics, Peking University, Beijing, China*

Abstract

This paper reports the design and fabrication of a low-voltage lateral-contact microrelay for RF applications. The silicon surface micromachined relay utilizes electrothermal actuators and low-stress silicon nitride as a structural connection as well as electrical and thermal isolation. The sidewall contact is sputtered gold. The driving voltage is measured to be as low as 8 V. RF testing shows that the microrelay has an off-state isolation of −20 dB at 12 GHz. The simplicity of this four-mask fabrication process provides the possibility of integration with other passive RF MEMS components.

Keywords: Microrelay; RF switch; Lateral contact; Low voltage; Electrothermal actuator

1. Introduction

With the recent progress of microelectromechanical system (MEMS) technology, more and more attention has been focused on the development of MEMS devices for RF applications. MEMS switches are one of the most promising future micromachined products that have attracted numerous research efforts in recent years. They have many potential applications including signal routing in RF system front-ends, impedance matching networks, switched filter banks and other high-frequency reconfigurable circuit applications. Compared to their conventional electromechanical or solid-state counterparts, micromachined relays offer many advantages in terms of low insertion loss, high off-state isolation and linearity, high breakdown voltage and integration capability. The majority of MEMS switches reported to date employs electrostatic actuation [1–4] and requires large actuation voltages. Few are lateral relays [5,6] and those often require non-standard post-process, and none of them have reported RF performance. For the conventional parallel-plate MEMS switches that utilize electrostatic actuation, a large enough closing gap to achieve high isolation usually results in an even larger driving voltage. In addition, the signal lines and the top plate have to be realized by two separate process steps.

In this paper, we present a lateral-contact microrelay fabricated on a silicon substrate using surface micromachining techniques. This relay is electrothermally actuated and exhibits excellent RF performance due to its lateral-contact mechanism. The microrelay consists of polysilicon and low-stress silicon nitride as structural materials and sputtered gold as the contact metal. Metal to metal contact is realized by in-plane motion and sidewall connection.

2. Design

Fig. 1 illustrates the operation principle of the microrelay. It utilizes V-shaped electrothermal actuators, for which extensive research has been conducted both theoretically and experimentally [7,8]. When a current flows through a V-shaped polysilicon beam, the thermal expansion caused by resistive heating actuates the rest of the suspended structure. A piece of silicon nitride serves as a structural connection between the polysilicon beams, as well as electrical and thermal isolation between the driving structure and the contact structure. The contact head, signal lines and their sidewalls are coated with gold. The in-plane motion of the actuator allows the contact head to move forward and connect the RF signal lines via sidewall contact.

☆ This paper was presented at the 15th IEEE MEMS conference, held in Las Vegas, USA, January 20–24, 2002, and is an expansion of the abstract as printed in the Technical Digest of this meeting.

* Corresponding author. Present address: Berkeley Sensor and Actuator Center, 497 Cory Hall, University of California, Berkeley, CA 94720, USA. Tel.: +1-510-375-1688; fax: +1-253-663-6323.
E-mail address: yw51@cornell.edu (Y. Wang).

0924-4247/03/$ – see front matter
PII: S0924-4247(02)00337-0

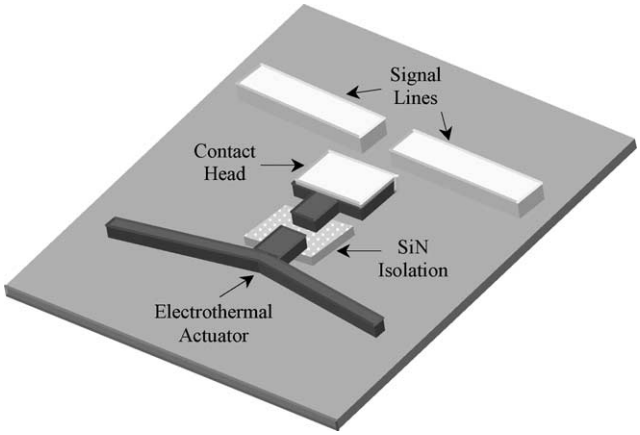

Fig. 1. Schematic illustration of the microrelay.

The advantage of electrothermal actuators compared to electrostatic actuation is mainly their IC-compatible driving voltages. For electrothermal actuators that provide planar motion, V-shaped actuator beams were chosen for their rectilinear displacements caused by resistive heating and their design simplicities and flexibilities. In addition, V-shaped actuators are capable of producing large output force from hundreds of micronewtons up to millinewton range. An output force of 8 mN can be achieved at an input power of 180 mW with 12 V bias as reported in [7]. This will be sufficient to provide a stable contact with low contact resistance in the range of milliohms [9].

Actuator beams of the same dimension are cascaded to produce larger displacement as depicted in Fig. 2. A current flow between terminals A and B will cause all three V-beams to expand due to resistive heating. The thermal expansion of the two side beams increases the vertical displacement (in y direction) of the center beam. This generates a larger deflection at the tip compared to a single actuator beam. The nominal dimension of a single actuator beam has a length of 200 μm, width and thickness of 2 μm and center offset of 10 μm. For a single V-beam actuator with nominal dimension, simulation in ANSYS shows that the maximum displacement at the tip is only 1.1 μm for a temperature increase of 500 K. For the arrangement in Fig. 2 where three V-beams of the same nominal dimensions are cascaded together, the displacement is calculated to be 4.8 μm—a significant increment over that of the single V-beam.

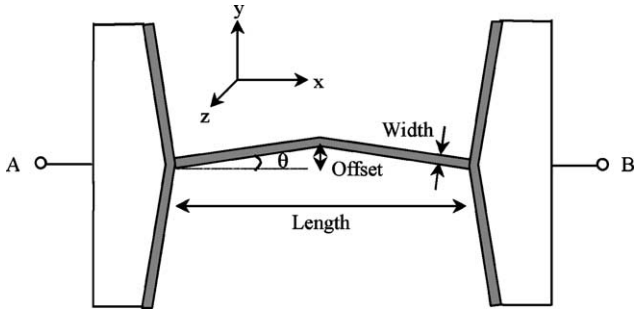

Fig. 2. Schematic diagram of the cascaded thermal actuator beams (top view).

For a single V-shaped actuator beam, the spring constant in the y direction (in-plane) is given in [7] as

$$K_y = \frac{4\sin^2(\theta')WtE}{L} \tag{1}$$

where L and W are the length and width as defined in Fig. 2; t the beam thickness and E the Young's modulus. θ' is the effective bending angle due to expansion and it is approximated as the bending angle θ, which is also defined in Fig. 2. Eq. (1) yields a y-directional spring constant of 134.9 N/m. ANSYS simulation shows a spring constant $K_y = 129.5$ N/m, which is within 4% of the calculated value. This is consistent with the results given in [7]. For the tri-beam geometry, the simulation gives spring constants as $K_y = 6.67$ and $K_z = 1.78$ N/m. For the smallest spring constant, a mechanical resonant frequency of 42.3 KHz can be found, which indicate good mechanical robustness. This is partly due to the extremely small mass of the suspended structure.

The microrelay itself occupies an area of 200 μm × 220 μm excluding the RF lines and testing pads. Test structures of cascaded actuator beams with various dimensions were designed and simulated. Table 1 shows the design values and ANSYS simulation of their displacements under a given thermal load. Type 1 design gives the nominal dimension.

Gold was chosen as the contact metal because of its low resistivity, good stability and efficiency in RF signal propagation. Its skin depth can be calculated by

$$\delta = \frac{1}{\sqrt{f2\pi\sigma}} = \sqrt{\frac{\rho}{\pi\mu_0 f}} \tag{2}$$

where the resistivity of gold $\rho_{Au} = 2.4\,\mu\Omega\,\text{cm}$ and $\mu_0 = 4\pi \times 10^{-7}$ H/m. This gives a skin depth of 0.71 μm at 12 GHz. Sputtering is selected as method of metal deposition instead of evaporation in order to ensure good sidewall coverage. Meanwhile, sputtered gold is known to have higher hardness which gives less surface damage for metallic microcontacts [9].

Different contact head shapes including round, square and angled have been designed to explore their reliabilities. Contact head areas between 700 and 1200 μm^2 were

Table 1
Various actuator test structures and their simulated displacements

	Length (μm)	Width (μm)	Offset (μm)	Displacement (μm)
Type 1	200	2	10	5.4
Type 2	240	2	10	7.2
Type 3	240	1	15	6.2
Type 4	260	1.5	10	7.9
Type 5	280	2	10	8.6
Type 6	300	2	15	9.2

designed after considering the tradeoff between contact resistance and the load the contact head puts on the extension beams. The closing gap between the contact head and the signal lines was about 4–5 μm to ensure good sidewall coverage of the sputtered gold in the trench. After sputtering the gap distance is reduced by approximately 1 μm.

3. Fabrication

Fig. 3 shows the cross-sectional schematic illustration of the fabrication sequence. The process starts with a silicon wafer with resistivity of 10 Ω cm and thickness of 525 μm. First, the substrate is thermally oxidized at 1000 °C to grow a layer of silicon dioxide of 300 nm, followed by a deposition of 0.6 μm low-pressure chemical-vapor-deposited (LPCVD) low-stress silicon nitride at temperature of 850 °C. The SiO_2 and Si_3N_4 form an insulation layer to reduce substrate parasitics at high frequency due to the lossy nature of the silicon substrate. Then 2 μm of sacrificial

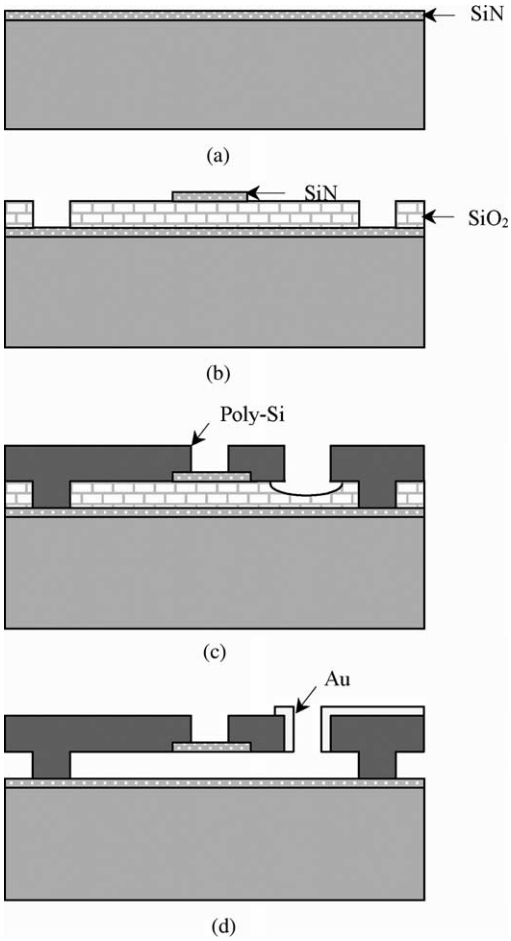

Fig. 3. Cross-sectional illustration of the process flow: (a) deposition of the low-stress Si_3N_4 as isolation; (b) deposition and patterning of sacrificial SiO_2 and low-stress Si_3N_4 connection; (c) deposition and patterning of poly-Si and partial release; (d) sputtering and lift-off of Au and HF release.

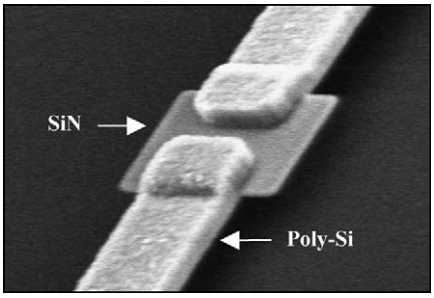

Fig. 4. SEM image of the Si_3N_4 structure connecting two polysilicon structures.

low-temperature oxide (LTO) is deposited and anchors are patterned. Afterwards another 0.6 μm of LPCVD low-stress silicon nitride is deposited and patterned. It serves as the structural connection as well as the electrical and thermal isolation between the driving structure and the contact structure. Fig. 4 shows an SEM micrograph of a piece of silicon nitride connecting two polysilicon structures. No bending of the suspended polysilicon structure was observed, which indicates the stress mismatch between polysilicon and low-stress silicon nitride is negligible.

Next, 2 μm of in situ doped n-type polysilicon film is deposited at 620 °C. It is patterned using 0.4 μm oxide as hard mask. A partial release step is performed by dipping the wafer into 6:1 BHF, exposing only the small region between the contact head and the RF signal lines. Approximately 0.5–0.7 μm of the sacrificial oxide in the closing gap area is removed to ensure the separation of sputtered gold on the contact head sidewalls and the signal lines, as well as the removal of unwanted gold in the area between them. A thin layer of gold (0.3–0.5 μm) is then sputtered and lifted off, leaving gold only on the contact sidewalls and signal routing lines. Fig. 5 shows a uniform coverage of gold on the contact head and signal lines with a close-up image of the gold coating on the sidewalls. Finally, the device is released in concentrated HF acid for 5–7 min and the polysilicon and silicon nitride structures are suspended above the substrate. A supercritical CO_2 drying after HF release is helpful to reduce the surface stiction of the thin actuator beams.

A fabricated microrelay with square-shaped contact is shown in Fig. 6. The fabrication is completed using standard MEMS processes with only four masks including lift-off. No post-processing is required. Contact metal is realized in one-step lithography and gold sputtering. The simplicity of this process allows design flexibility, and possible integration of this microrelay with other passive RF MEMS components.

4. Results and discussion

4.1. Electrical testing

Electrical testing was done using an HP 4145B parameter analyzer at room temperature in an air ambient environment.

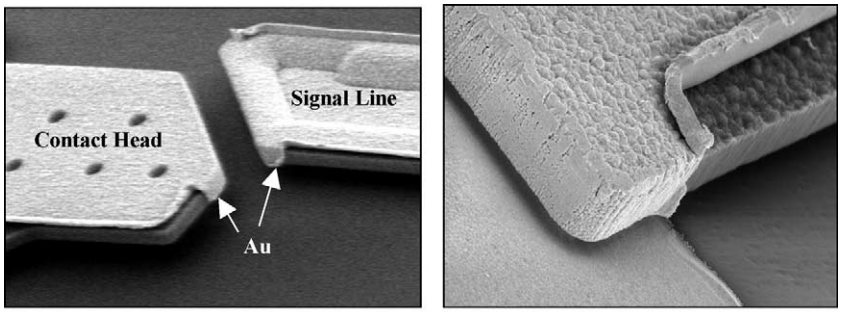

Fig. 5. (a) SEM image of the contact sidewalls coated with Au; (b) close-up image of the Au coating (warpage is due to lift-off).

It shows that the microrelay can be operated at voltages of 8–15 V. Depending on the applied voltage, the relay's contact resistance varies from 0.5 to 3.6 Ω. The driving voltage can be further reduced by decreasing the closing gap between the contact head and the signal lines. During the microrelay's on state, the power consumption of the thermal actuator is in the range 20–40 mW. The break down voltage of the signal path is measured to be as high as 500 V.

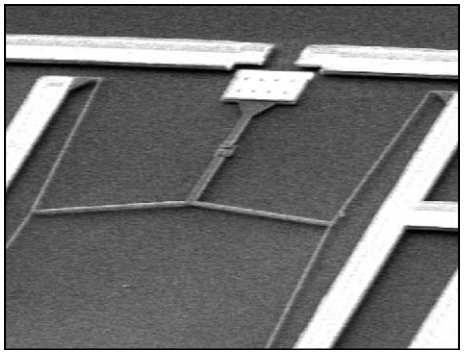

Fig. 6. SEM image of the fabricated microrelay with square-shaped contact head.

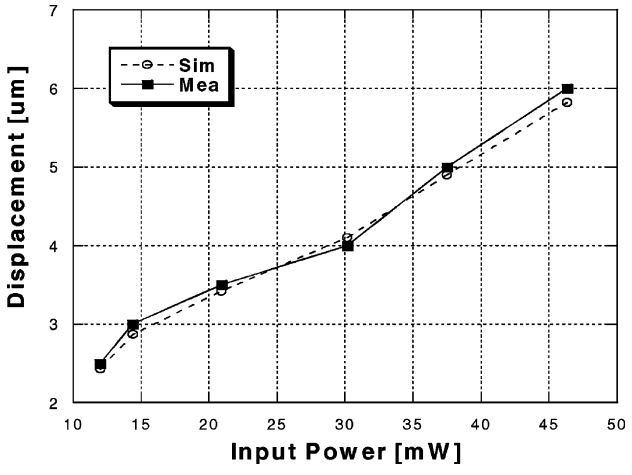

Fig. 7. Measured actuator displacements versus simulated values at various input power.

The measured actuation displacements at different input powers for the actuator beam arrays with nominal dimension are plotted in Fig. 7. Simulation parameters were adjusted to account for their changes due to thermal heating. This gives good agreement between the measured displacement and simulation, which shows a linear proportion to the input power. Test structures listed in Table 1 were examined and their actuation distances were compared with ANSYS simulations.

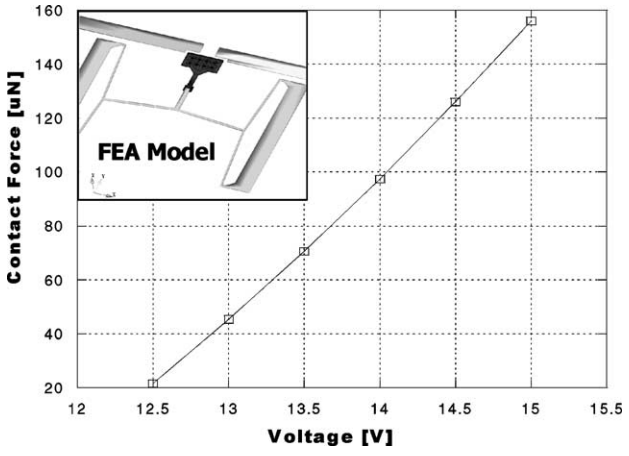

Fig. 8. Simulated contact force versus applied voltage.

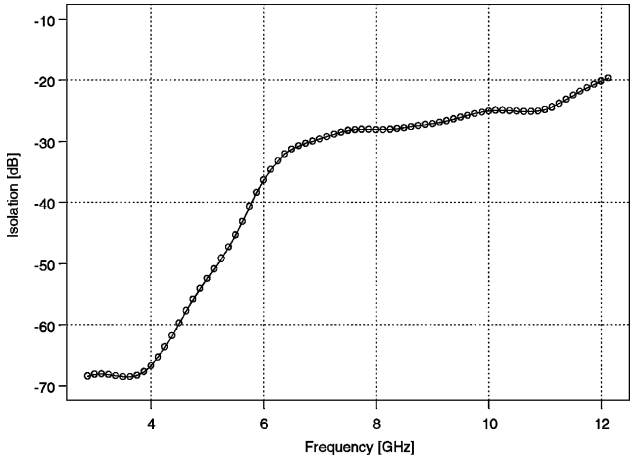

Fig. 9. Measured relay off-state isolation.

Table 2
Comparison of selected recent MEMS relays and this design

Reference	Motion	Substrate	Contact	Voltage (V)	Isolation
[1]	Vertical	GaAs	Ohmic	5	−30 dB at 4 GHz
[2]	Vertical	GaAs	Capacitive	8	−42 dB at 5 GHz
[3]	Vertical	Si	Ohmic	10	−8 dB at 6 GHz
[4]	Vertical	GaAs	Ohmic	70	−30 dB at 40 GHz
This design	Lateral	Si	Ohmic	8	−20 dB at 12 GHz

Contact force is critical in determining microrelay's on-resistance. A contact force between 50 and 200 μN is needed to generate a contact resistance of 100–300 mΩ according to [9]. A FEM analysis tool-CoventorWare was used to simulate the contact force generated by the cascaded V-beam actuator at each driving voltage. Fig. 8 shows the plotted results. The contact force is computed to be 21.57 μN for 12.5 V and 156.05 μN for 15 V.

4.2. RF testing

RF testing was performed using an HP 8510C network analyzer and coplanar ground–signal–ground (GSG) probes with 150 μm pitch. Two-port S-parameters were measured and shunt parasitics of the RF testing structures were de-embedded to obtain the performance of device under test (DUT). Fig. 9 shows the measured off-state isolation is as high as −20 dB at 12 GHz. The measurements also indicate the microrelay has an insertion loss of less than −1 dB at 12 GHz with most resistive loss occurs on the signal lines.

During microrelay's off state, the isolation is mainly determined by the capacitive coupling between the signal lines. In our case, it is dominated by substrate parasitics due to the lossy nature of the silicon wafer. RF signal lines with 20 μm width are separated by a distance of 22 μm for the case of square-shaped contact. The closing gap between the contact head and RF lines is around 3–4 μm. Simulation in CoventorWare shows that the coupling capacitance between the signal lines through the contact head is 8.26 fF. It also verifies that the substrate parasitics account for 90% of the capacitance coupling between the signal lines. This gives a lot of room for improving the relay's isolation at high frequency by using high-resistive substrate or using thick passivation layer to reduce substrate leakage.

A comparison between some of the most recent RF switches and this design is tabulated in Table 2. It shows that the microrelay exhibits high isolation in the GHz frequency range comparable to those fabricated on GaAs substrate with similar actuation voltage.

Reliability studies of the microrelay show that metal-contact welding causes the most failures. Surface roughness on the sidewall may also result in poor contacts. The high adherence force of gold plays a role in the contact degradation as well. Gold and nickel alloy can be considered as an alternative choice of contact metal due to its improved hardness, a much smaller adherence force (one-ninth of that of gold) and relatively low resistivity [10]. Contact heads with round and square shape showed better reliability than the angle-shaped contact heads.

5. Conclusions

An electrothermally actuated lateral-contact microrelay for RF applications has been designed and fabricated on a silicon substrate using surface micromachining techniques. Low-stress silicon nitride used as a structural connection shows promising results with good electrical isolation and negligible stress mismatch. The lowest actuation voltage of the microrelay is 8 V. The microrelay has an off-state isolation of −20 dB at 12 GHz and low insertion loss of less than −1 dB. The lateral-contact mechanism of the microrelay provides a high RF performance. The measured off-state isolation in the GHz frequency range is comparable with some recently reported RF MEMS switches fabricated on semi-insulating substrate. The simplicity of the fabrication process enables the possible integration of the microrelay with other passive RF MEMS components.

Acknowledgements

The authors would like to thank Prof. Edwin Kan for providing the testing equipment and the staff of Cornell Nanofabrication Facility. The authors would also like to thank A. Yeh, H. Jiang, K. Yoo and Z. Liu for their fruitful discussions.

References

[1] D. Hah, E. Yoon, S. Hong, A low-voltage actuated micromachined microwave switch using torsion springs and leverage, IEEE Trans. Microwave Theory Tech. 48 (12) (2000) 2540–2545.
[2] J.Y. Park, G.H. Kim, K.W. Chung, J.U. Bu, Monolithically integrated micromachined RF MEMS capacitive switches, Sens. Actuators A 89 (2001) 88–94.
[3] F. Plotz, S. Michaelis, G. Fattinger, R. Aigner, R. Noe, Performance and dynamics of a RF MEMS switch, in: Proceedings of the Transducers'01, Munich, Germany, 2001, pp. 1560–1563.
[4] R.E. Mihailovich, M. Kim, J.B. Hacker, E.A. Sovero, J. Studer, J.A. Higgins, J.F. deNatale, MEM relay for reconfigurable RF circuits, IEEE Microw. Wireless Compon. Lett. 11 (2) (2001) 53–55.

[5] E.J.J. Kruglick, K.S.J. Pister, Lateral MEMS microcontact considerations, IEEE J. Microelectromech. Syst. 8 (3) (1999) 264–271.
[6] J. Simon, S. Saffer, F. Sherman, C.-J. Kim, Lateral polysilicon microrelays with a mercury microdrop contact, IEEE Trans. Indus. Electr. 45 (6) (1998) 854–860.
[7] L. Que, J.-S. Park, Y.B. Gianchandani, Bent-beam electrothermal actuators. Part I. Single beam and cascaded devices, IEEE J. Microelectromech. Syst. 10 (2) (2001) 247–262.
[8] J.M. Maloney, D.L. DeVoe, D.S. Schreiber, Analysis and design of electrothermal actuators fabricated from single crystal silicon, in: Proceedings of the ASME International Mechanical Engineering Congress and Exposition, 2000, pp. 233–240.
[9] D. Hyman, M. Mehregany, Contact physics of gold microcontacts for MEMS switches, IEEE Trans. Compon. Pack. Technol. 22 (3) (1999) 357–364.
[10] J. Schimkat, Contact materials for microrelays, in: Proceedings of the IEEE 11th Annual International Workshop on Microelectromechanical Systems, Heidelberg, Germany, 1998, pp. 190–194.

Biographies

Ye Wang received the BS degree in Electrical Engineering from University of Houston in 1998, and the MS degree in Electrical Engineering from Cornell University in 2001. She is currently working towards a PhD degree in Electrical Engineering also from Cornell University. Her research interests include design and fabrication of RF switches/microrelays and other passive RF MEMS on-chip components and their applications in wireless communication systems.

Zhihong Li was born in Changchun Province, China, in 1969. He received a BS degree from Department of Computer Science and Technology, Peking University, China, in 1992. He received a PhD degree at the Institute of Microelectronics, Peking University, majoring VLSI technology and reliability, in 1997. He is working at this institute in charge of design and fabrication of microelectromechanical systems (MEMS), especially RF MEMS. He is now a postdoctoral researcher at the Department of Electrical and Computer Engineering, University of California, Davis. Dr. Li is a member of IEEE.

Daniel T. McCormick received the BSE degree in Biomedical Engineering and in Electrical Engineering from Duke University in 1999, and the MS degree in Electrical Engineering from Cornell University in 2002. He is currently a PhD candidate at Cornell University in the field of Electrical and Computer Engineering. His primary research interests are in the design and fabrication of biomedical MEMS for medical imaging and diagnostics as well as RF MEMS.

Norman C. Tien is a professor in the Department of Electrical and Computer Engineering at the University of California at Davis where his research interest is the development of silicon microelectromechanical systems (MEMS), particularly for applications in information technology. He is also a co-Director of the Berkeley Sensor and Actuator Center. Tien was a faculty at Cornell University from 1996 to 2000, where he became an associate professor in the School of Electrical and Computer Engineering. From 1993 to 1996, he was a lecturer in the Department of Electrical Engineering and Computer Science at the University of California, Berkeley, and a postdoctoral research engineer at the Berkeley Sensor and Actuator Center. Tien is an editor of the IEEE/ASME Journal of Microelectromechanical Systems. In 2000, he co-founded AIP Networks, an optical network components company. Dr. Tien received a BS degree from the University of California, Berkeley, a MS degree from the University of Illinois, Urbana-Champaign, and a PhD from the University of California, San Diego.